

Synthesis and absorption properties of some new azo-metal chelates and their ligands

Haifeng Song, Kongchang Chen, Dongqing Wu, He Tian*

Institute of Fine Chemicals, East China University of Science and Technology, Shanghai 200237, P.R. China

Received 13 February 2003; received in revised form 12 May 2003; accepted 9 July 2003

Abstract

Some new azo-metal chelates were synthesized using different diazo components, coupling components and metal ions. Their structures were confirmed by IR spectra, MS spectra and UV–Vis spectra. Their solubility in 4-hydroxy-4-methyl-2-pentanone and absorption properties of film were measured. The influence on the difference of absorption maximum from azo-metal chelates to their ligands by diazo components, coupling components and metal ions was studied.

© 2003 Elsevier Ltd. All rights reserved.

Keywords: Azo-metal chelate; Ligand; Absorption spectra; Synthesis

1. Introduction

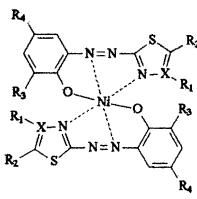
In recent years, azo-metal chelates have been studied widely because of their excellent thermal and optical properties in the applications such as optical recording medium [1–6], toner [7,8], ink-jet printing [9,10] and oil-soluble lightfast dyes [11] and so on. But these works paid their main attention to the synthesis of the dyes, and there have been little study work on the relationships between the difference ($\Delta\lambda_{\text{max}}$) of absorption maximum from azo-metal chelates to their ligands and the structures of the azo-metal chelates. In fact, the study work on these relationships is as important as the synthesis of the dyes. According to the relationships (if possible to be revealed clearly in

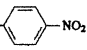
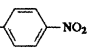
this work), we can estimate the absorption maximum of azo-metal chelates on the basis of that of their ligands. Yagi [12,13] had studied the influence of metal ions on the change of absorption maximum from azo-metal chelates to their ligands, but he didn't study the influence of the structures of azo-metal chelates. In this work, we synthesized some new azo dyes and azo-metal chelates using different diazo, coupling components and metal ions. Their chemical structures are shown in Table 1. The relationships between the difference ($\Delta\lambda_{\text{max}}$) of absorption maximum from azo-metal chelates to their ligands and the structures of the azo-metal chelates were studied. It can be expected that these relationships will guide the synthesis of new azo dyes for the application later. Moreover, we also studied the solubility of these azo-metal chelates in 4-hydroxy-4-methyl-2-pentanone and the absorption maximum of their films. These

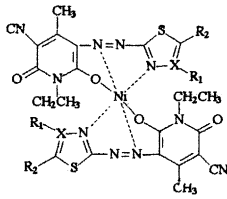
* Corresponding author. Fax: +86-21-64252288.
E-mail address: tianhe@ecust.edu.cn (H. Tian).

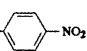
Table 1

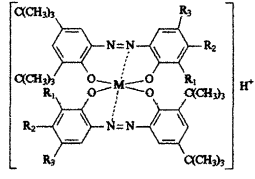
Chemical structures of azo-metal chelates in the study



Dye No.	X	R ₁	R ₂	R ₃	R ₄
1	N	—	H	—C(CH ₃) ₃	—C(CH ₃) ₃
2	N	—	—CH ₃	—C(CH ₃) ₃	—C(CH ₃) ₃
3	C		H	—C(CH ₃) ₃	—C(CH ₃) ₃
4	N	—	H	H	—C(CH ₃) ₃
5	N	—	—CH ₃	H	—C(CH ₃) ₃
6	C		H	H	—C(CH ₃) ₃



Dye No.	X	R ₁	R ₂
7	N	—	H
8	N	—	—CH ₃
9	C		H



Dye No.	R ₁	R ₂	R ₃	M
10	H	H	—SO ₂ N(CH ₂ CH ₃) ₂	Cr
11	—SO ₂ NH ₂	H	—CH ₃	Cr
12	H	—NO ₂	H	Cr
22	—SO ₂ NH ₂	H	—CH ₃	Co

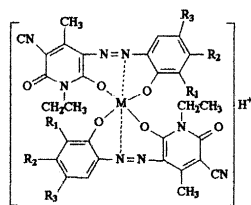
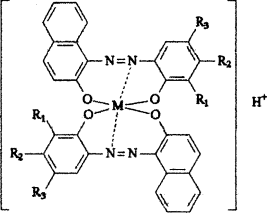
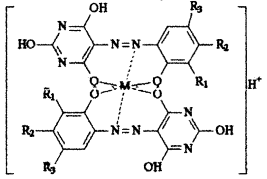


Table 1 (continued)

13	H	H	$-\text{SO}_2\text{N}(\text{CH}_2\text{CH}_3)_2$	Cr
14	$-\text{SO}_2\text{NH}_2$	H	$-\text{CH}_3$	Cr
15	H	$-\text{NO}_2$	H	Cr
23	H	H	$-\text{SO}_2\text{N}(\text{CH}_2\text{CH}_3)_2$	Co
				
16	H	H	$-\text{SO}_2\text{N}(\text{CH}_2\text{CH}_3)_2$	Cr
17	$-\text{SO}_2\text{NH}_2$	H	$-\text{CH}_3$	Cr
18	H	$-\text{NO}_2$	H	Cr
				
19	H	H	$-\text{SO}_2\text{N}(\text{CH}_2\text{CH}_3)_2$	Cr
20	SO_2NH_2	H	$-\text{CH}_3$	Cr
21	H	$-\text{NO}_2$	H	Cr
24	$-\text{SO}_2\text{NH}_2$	H	$-\text{CH}_3$	Co

properties are very important for the application of azo-metal chelates as optical recording medium.

2. Experimental

IR spectra of the dyes were carried out on a Nicolet 55XC instrument using KBr tabulating. ^1H -NMR spectra were measured on Brüker AVANCE 500 at 500 MHz in deuterium solvent, with TMS as an internal reference. ESI mass spectra (70 eV) were recorded on a Micromass LCT spectrometer. Visible absorption spectra were recorded on a Shimadzu UV-260 spectrophotometer.

2-Amino-1,3,4-thiadiazole was prepared from thiosemicarbazide and formic acid using the method described in the literature [14]. 2-Amino-5-methyl-1,3,4-thiadiazole was prepared from thiosemicarbazide and acetic acid using the method described in the literature [15]. 2-Amino-4-(4'-

nitro-phenyl)-thiazole was prepared from thiourea and 4-nitroacetophenone using the method described in the literature [16]. 1-Ethyl-3-cyano-6-hydroxy-4-methyl-2-pyridone was prepared from ethyl acetoacetate, cyano-acetate and ethylamine using the method described in the literature [17].

2.1. Diazotisation of 2-amino-1,3,4-thiadiazole, 2-amino-5-methyl-1,3,4-thiadiazole and 2-amino-4-(4'-nitro-phenyl)-thiazole [18]

2-amino-1,3,4-thiadiazole (or 2-amino-5-methyl-1,3,4-thiadiazole, 2-amino-4-(4'-nitro-phenyl)-thiazole) (0.10 mol) was dissolved in the solution containing 10 ml of acetic acid and 5 ml propionic acid. Sulfuric acid (1 ml) was dropwise added at a temperature of from -5 to 0°C , and then 3.55 g of 43% nitrosyl sulfuric acid was added at a temperature of from -5 to 0°C , followed by stirring for 2 h.

2.2. Diazotisation of 2-methoxy-4-(*N,N*-diethyl)sulfanilamide-aniline, 2-methoxy-3-sulfanilamide-4-methyl-aniline and 2-methoxy-4-nitro-aniline

Substituted aniline (0.01 mol) was dissolved in the solution containing 20 ml of water and 3 ml of 37% hydrochloric acid, then 2.1 g of 33% sodium nitrite water solution was dropwise added at a temperature of from -5 to 0 °C, then followed by stirring for 1 h.

2.3. General preparation procedure of ligands

Coupling component (0.01 mol) was dissolved in sodium hydrate solution (20 ml water, 20 ml ethanol and 0.02 mol sodium hydrate) and cooled to -5 – 0 °C in an ice salt bath. The diazo salt solution was stirred into the coupling component solution. During the procedure, the pH value was maintained within 9–12, the temperature within -5 – 0 °C. The mixture was stirred for 4 h, then the pH value was regulated to 6–7, further stirred for 1 h and then filtered. The solid was washed with water and recrystallized with ethanol.

2.4. General preparation procedure of nickel azo chelates [18]

The ligand (0.01 mol) was dissolved in 50 ml of methanol, and a solution having 1.24 g of nickel acetate tetrahydrate dissolved in 15 ml of methanol was added into it at room temperature. Then, the mixture was stirred at room temperature for 3 h, and 50 ml of water was added. Precipitated crystals were collected by filtration and dried to obtain a nickel chelate compound. The solid was purified by column chromatography.

2.5. General preparation procedure of chromium and cobalt azo chelates

The ligand (0.01 mol) was dissolved in 50 ml of *N,N*-dimethylformamide, and then the solution was heated to 100 °C. A solution having 1.33 g of chromium (III) chloride hexahydrate or 1.25 g of cobalt acetate tetrahydrate dissolved in 10 ml of *N,N*-dimethylformamide was added into it at this

temperature. Then the mixture was refluxed for 6 h. *N,N*-dimethylformamide (40 ml) was evaporated out, the mixture was cooled to the room temperature. Precipitated crystals were collected by filtration and dried to obtain metal chelate compound, which was purified by column chromatography.

3. Results and discussion

3.1. Structure identification of ligands and azo-metal chelates

The structures of ligands were confirmed by ^1H -NMR. The structure data for some typical ligands were listed in Table 2. FT-IR spectra and MS spectra confirmed the structures of azo-metal chelates. IR spectra of azo-metal chelate **10** and its ligand were shown in Fig. 1 and MS spectra data for some typical azo-metal chelates were listed in Table 3. From Fig. 1, we can see the presence of the coordination sites of azo-metal chelate. While a broad hydroxyl ($-\text{OH}$) at 3433 cm^{-1} , a sharp azyl ($-\text{N}=\text{N}-$) peak at 1484 cm^{-1} and a sharp methoxy ($-\text{OCH}_3$) peak at 1279 cm^{-1} were observed in the IR spectra of ligand, there were no such peaks in the spectra of azo-metal chelate. The broad peak at 3451 cm^{-1} in the IR spectra of azo-metal chelate might be caused by water. As seen from MS spectra data listed in Table 3, there was $(\text{M}+23)^+$ peak or $(\text{M}+45)^+$ peak for some azo-metal chelates. The reason was followed:

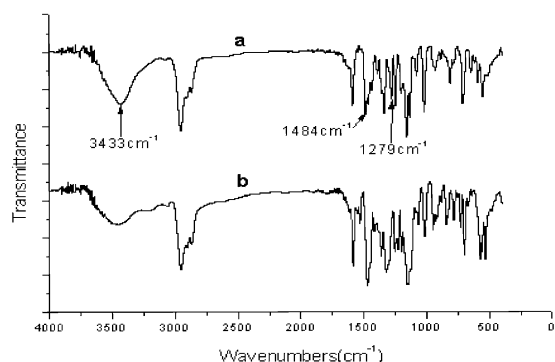


Fig. 1. IR spectra of azo-metal chelate **10** and its ligand (a, ligand; b, azo-metal chelate).

$(M+23)^+$ peak was caused by the sodium ion, because some sodium salt was added in order to increase the ionization degree when the sample was analyzed. Chromium or cobalt azo chelates were prepared in *N,N*-dimethylformamide by refluxing. Some *N,N*-dimethylformamide would be decomposed to dimethylamine at so high temperature which formed salt with azo-metal chelates, which could result in $(M+45)^+$ peak in the MS spectra. The formation of a metal chelate was also confirmed by UV–Vis spectra. For example, in the normalized UV–Vis spectra for azo-metal chelates **5**, **18**, **23** shown in Figs. 2–4, λ_{\max} were

597.6, 594.8, and 478.6 nm for azo-metal chelates respectively, while 343.2, 497.4, and 439.8 nm for their ligands respectively. The absorption spectra of azo-metal chelates showed a red shift compared with that of their ligands.

3.2. Absorption spectra

In order to supply guiding help for the synthesis later, we studied the relationships between the difference ($\Delta\lambda_{\max}$) of absorption maximum from azo-metal chelates to their ligands and the structures of the azo-metal chelates.

Table 2
Yields and characterization data for some typical ligands

Ligand ^a No.	Yield (%)	Melting point (°C)	¹ H-NMR (ppm)
I (1)	70	188–190	1.37(s, 9H, $-\text{C}(\text{CH}_3)_3$), 1.46(s, 9H, $-\text{C}(\text{CH}_3)_3$), 7.60(s, 1H, Ar-H), 7.70(s, 1H, Ar-H), 9.12(s, 1H, Ar-H)
II (3)	65	215–218	1.38(s, 9H, $-\text{C}(\text{CH}_3)_3$), 1.47(s, 9H, $-\text{C}(\text{CH}_3)_3$), 7.58(s, 1H, Ar-H), 7.72(s, 1H, Ar-H), 7.76(s, 1H, Ar-H), 8.15 (d, 2H, $J=8.83$ Hz, Ar-H), 8.34(d, 2H, $J=8.68$ Hz, Ar-H)
III (5)	75	123–125	1.37(s, 9H, $-\text{C}(\text{CH}_3)_3$), 2.86(s, 3H, $-\text{CH}_3$), 7.04(d, 1H, $J=8.70$ Hz, Ar-H), 7.55(d, 1H, $J=8.67$ Hz, Ar-H), 7.85(s, 1H, Ar-H)
IV (8)	85	> 300	1.11(t, 3H, $J=6.99$ Hz, 7.03 Hz, $-\text{CH}_2\text{CH}_3$), 2.49(s, 3H, $-\text{CH}_3$), 2.66(s, 3H, $-\text{CH}_3$), 3.94(m, 2H, $-\text{CH}_2-$)
V (10)	90	153–154	1.15(t, 6H, $J=7.25$ Hz, 7.10 Hz, $-\text{N}(\text{CH}_2\text{CH}_3)_2$), 1.39(s, 9H, $-\text{C}(\text{CH}_3)_3$), 1.47(s, 9H, $-\text{C}(\text{CH}_3)_3$), 3.27(m, 4H, $-\text{CH}_2-$), 7.16(d, 1H, $J=8.77$ Hz, Ar-H), 7.46(s, 1H, Ar-H), 7.81(s, 1H, Ar-H), 7.86(d, 1H, $J=8.73$ Hz, Ar-H), 8.30(s, 1H, Ar-H)
VI (11)	89	232–233	1.39(s, 9H, $-\text{C}(\text{CH}_3)_3$), 1.48(s, 9H, $-\text{C}(\text{CH}_3)_3$), 2.68(s, 3H, $-\text{CH}_3$), 4.1(s, 3H, $-\text{OCH}_3$), 7.56(s, 1H, Ar-H), 7.83(m, 3H, Ar-H)
VII (12)	92	216–217	1.39(s, 9H, $-\text{C}(\text{CH}_3)_3$), 1.48(s, 9H, $-\text{C}(\text{CH}_3)_3$), 4.28(s, 3H, $-\text{OCH}_3$), 7.36(s, 1H, Ar-H), 7.60(s, 1H, Ar-H), 7.79(s, 1H, Ar-H), 8.01(d, 1H, $J=8.89$ Hz, Ar-H), 8.07(d, 1H, $J=8.84$ Hz, Ar-H)
VIII (13)	88	233–235	1.17(t, 6H, $J=7.22$ Hz, 7.15 Hz, $-\text{N}(\text{CH}_2\text{CH}_3)_2$), 1.25(t, 3H, $J=8.04$ Hz, 6.09 Hz, $-\text{CH}_2\text{CH}_3$), 3.28(m, 4H, $-\text{N}(\text{CH}_2\text{CH}_3)_2$), 4.06(m, 2H, $-\text{CH}_2-$), 7.08(d, 1H, $J=8.71$ Hz, Ar-H), 7.70(d, 1H, $J=7.70$, Ar-H), 8.11(s, 1H, Ar-H)
IX (16)	91	201–202	1.16(t, 6H, $J=7.12$, 7.12 Hz, $-\text{CH}_3$), 3.31(m, 4H, $-\text{CH}_2-$), 4.17(s, 3H, $-\text{OCH}_3$), 6.77(d, 1H, $J=9.6$ Hz, Ar-H), 7.40(d, 1H, $J=8.68$ Hz, Ar-H), 7.48(t, 1H, $J=7.15$, 7.29 Hz, Ar-H), 7.63(t, 1H, $J=7.19$, 8.16 Hz, Ar-H), 7.72(m, 2H, Ar-H), 7.90(d, 1H, $J=9.60$ Hz, Ar-H), 8.38(s, 1H, Ar-H), 8.49(d, 1H, $J=8.15$ Hz, Ar-H)
X (17)	90	258–260	2.72(s, 3H, $-\text{CH}_3$), 4.08(s, 3H, $-\text{OCH}_3$), 6.71(d, 1H, $J=9.64$ Hz, Ar-H), 7.36(s, 1H, Ar-H), 7.46(t, 1H, $J=7.47$, 7.46 Hz, Ar-H), 7.59(t, 1H, $J=7.17$, 8.19 Hz, Ar-H), 7.69(d, 1H, $J=7.57$ Hz, Ar-H), 7.88(d, 1H, $J=9.63$ Hz, Ar-H), 8.05(s, 1H, Ar-H), 8.54(d, 1H, $J=6.70$ Hz, Ar-H)
XI (19) ^a	95	271–274	1.10(t, 6H, $J=7.16$ Hz, 7.12 Hz, $-\text{N}(\text{CH}_2\text{CH}_3)_2$), 3.23(m, 4H, $-\text{N}(\text{CH}_2\text{CH}_3)_2$), 4.10(s, 3H, $-\text{OCH}_3$), 7.37(d, 1H, $J=8.65$ Hz, Ar-H), 7.67(d, 1H, $J=8.67$ Hz, Ar-H), 8.18(s, 1H, Ar-H)

^a The number in parentheses is the number of the azo-metal chelate prepared from the relevant ligand.

3.2.1. The influence on $\Delta\lambda_{\max}$ by the diazo components

The absorption spectra data of azo-metal chelates in ethanol were listed in Table 4 for five series (Series A–E). Coupling components of azo-metal

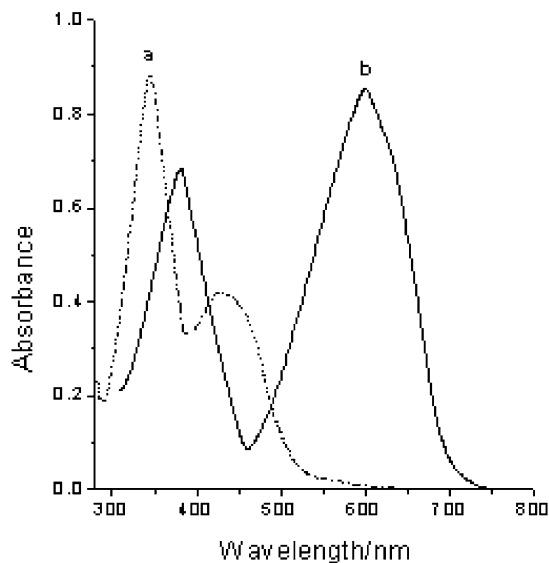


Fig. 2. Absorption of azo-metal chelate **5** and its ligand (a, ligand; b, azo-metal chelate).

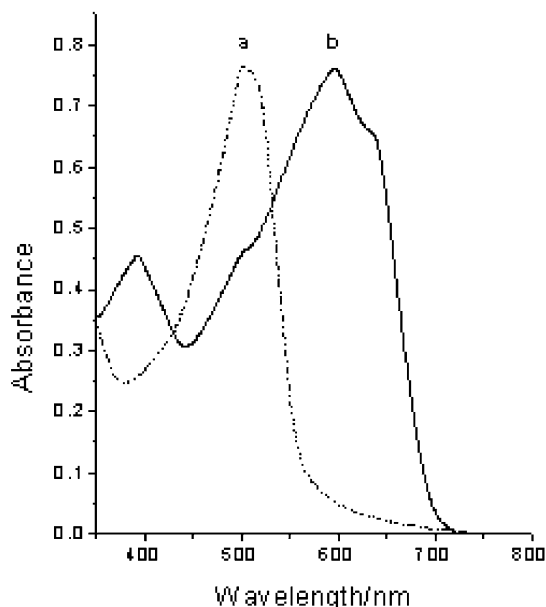


Fig. 3. Absorption of azo-metal chelate **18** and its ligand (a, ligand; b, azo-metal chelate).

chelates in every series were same. For example, coupling components of Series A and D, Series B, Series C and Series E were 2,4-ditertbutylphenol, 4-tertbutylphenol, barbituric acid and 2-naphthol respectively. But diazo components of them were different between azo-metal chelates in the same series. The results in Table 4 showed: when the absorption maximum of azo-metal chelates in the same series were increasing, $\Delta\lambda_{\max}$ were also increasing. Azo-metal chelates in every series were all in agreement with this trend. That is, $\Delta\lambda_{\max}$ was increasing with the increase of electron-drawing force of diazo component.

3.2.2. The influence on $\Delta\lambda_{\max}$ by the coupling components

The absorption spectra data of azo-metal chelates in ethanol were listed in Table 5 for three series (Series F–H). Diazo components of azo-metal chelates in every series were same. For example, diazo components of Series F, Series G and Series H were 2-amino-1,3,4-thiadiazole, 2-amino-5-methyl-1,3,4-thiadiazole and 2-amino-4-(4'-nitro-phenyl)-thiazole respectively. But coupling components of them were different between azo-metal chelates in the same series. From the

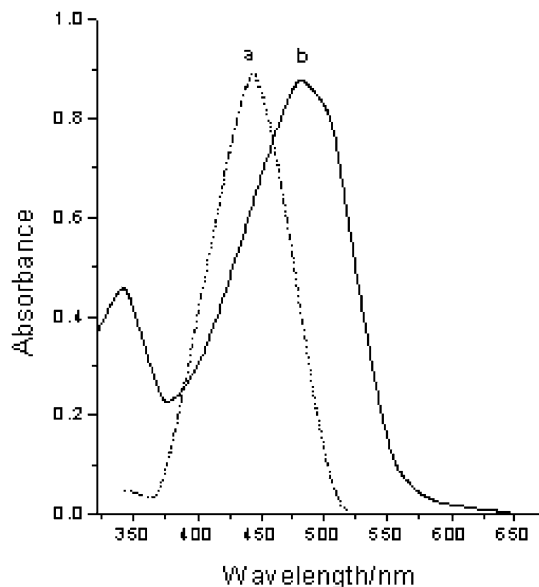


Fig. 4. Absorption of azo-metal chelate of **23** and its ligand (a, ligand; b, azo-metal chelate).

Table 3
Yields and mass spectra data for some typical azo-metal chelates

Dye No.	Yield (%)	Mw	MS m/z (rel. int.)	Dye No.	Yield (%)	Mw	MS m/z (rel. int.)
1	92	693.0	693.0 (100)	12	95	791.0	814.3 (4.83) (M + Na) ⁺ 792.3 (1.95)
2	91	720.7	743.2 (59.9) (M + Na) ⁺ 721.2 (23.3)	13	92	915.0	960.2 (100) (M + HN(CH ₃) ₂) ⁺
3	90	933.7	933.1 (100)	14	90	831.0	876.1 (0.49) (M + HN(CH ₃) ₂) ⁺
4	93	581.3	581.1 (43.9)	15	88	735.0	781.2 (100) (M + HN(CH ₃) ₂) ⁺ 758.1 (67.8) (M + Na) ⁺ 736.1 (46.4)
5	90	608.7	609.1 (19.5)	17	96	763.0	808.0 (100) (M + HN(CH ₃) ₂) ⁺ 786.0 (82.4) (M + Na) ⁺ 764.0 (14.0)
6	89	820.7	843.1 (100) (M + Na) ⁺ 821.1 (3.17)	18	94	669.0	712.0 (3.96) (M + HN(CH ₃) ₂) ⁺ 690.0 (0.95) (M + Na) ⁺ 669.0 (0.54)
9	85	876.7	899.1 (5.83) (M + Na) ⁺	20	93	731.0	775.9 (48.4) (M + HN(CH ₃) ₂) ⁺ 753.9 (100) (M + Na) ⁺ 732.0 (18.7)
10	94	971.2	993.3 (26.6) (M + Na) ⁺				

result we can see that the $\Delta\lambda_{\max}$ were increasing with the increase of absorption maximum of azo-metal chelates in the same series. Azo-metal chelates in every series were all in agreement with this trend.

Table 4
Influence on $\Delta\lambda_{\max}$ by the diazo components

Series No.	Dye No.	λ_{\max} (nm)	$\Delta\lambda_{\max}$ (nm)
A	1	608.4	253.4
	2	612.2	257.0
	3	621.8	296.0
B	4	564.2	249.8
	5	597.6	254.4
	6	602.6	281.4
C	10	553.2	186.2
	11	561.0	225.2
	12	599.2	235.4
D	16	563.0	69.4
	17	576.6	73.8
	18	594.6	97.4
E	19	475.0	74.6
	20	494.6	87
	21	502.8	87.6

That is, $\Delta\lambda_{\max}$ increases with the increasing of electron-pushing force of the coupling component.

The absorption spectra data of five series (Series C, A, E, I and J) azo-metal chelates were listed in Table 6, in which diazo components were different within the same series and coupling components were different for different series. Series C, A and E have been discussed before. Coupling compo-

Table 5
Influence on $\Delta\lambda_{\max}$ by the coupling components

Series No.	Dye No.	λ_{\max} (nm)	$\Delta\lambda_{\max}$ (nm)
F	7	477.0	45.4
	4	564.2	249.8
	1	608.4	253.4
G	8	471.0	42.4
	5	597.6	254.4
	2	612.2	257.0
H	9	487.6	40.0
	6	602.6	281.4
	3	621.8	296.0

nents of Series I and J were both 1-ethyl-3-cyano-6-hydroxy-4-methyl-2-pyridone. From the data we can see that when the electron-pushing force of coupling components decreases, the difference of $\Delta\lambda_{\max}$ between different azo-metal chelates in the same series also decreases obviously. For some

series, $\Delta\lambda_{\max}$ between different azo-metal chelates in it were almost the same within experimental error.

3.2.3. The influence on $\Delta\lambda_{\max}$ by metal ions

We also study the influence of different metal ions on $\Delta\lambda_{\max}$ for the same ligand. Yagi [12,13] had reported that the ability of metal ions to make red shift was $\text{Cr}^{3+} > \text{Co}^{3+}$. From Table 7, it is clearly shown that our results were in agreement with this conclusion. The results in our experiments can be explained as follows: after metal ion was connected with the oxygen atom of hydroxyl, the oxygen atom became easier to give unbonded electron to π -electron system, which made red shift of absorption of the dye. This ability increases with the increasing of the positive electricity ability of metal ion. The positive electricity ability of chromium ion is larger than that of cobalt ion, so the difference of absorption maximum of chromium azo chelates from azo-metal chelates to their ligands is larger than that of cobalt azo chelates.

3.3. Solubility of azo-metal chelates

The application of azo-metal chelates for optical recording medium has attracted chemists' interest

Table 6

Influence on $\Delta\lambda_{\max}$ by the coupling components

Series No.	Dye No.	$\Delta\lambda_{\max}$ (nm)
C	10	186.2
	11	225.2
	12	235.4
A	1	253.4
	2	257.0
	3	296.0
E	19	74.6
	20	87.0
	21	87.6
I	13	70.2
	14	69.6
	15	72.2
J	7	45.4
	8	42.4
	9	40.0

Table 7

Influence on $\Delta\lambda_{\max}$ by different metal ions

Dye No.	$\Delta\lambda_{\max}$ (nm)	Dye No.	$\Delta\lambda_{\max}$ (nm)	Dye No.	$\Delta\lambda_{\max}$ (nm)
11	225.2	13	70.2	20	87.0
22	192.6	23	38.8	24	58.6

Table 8

Solubility of some azo-metal chelates in 4-hydroxy-4-methyl-2-pentanone and absorption of them in the film

Dye No.	Solubility (%)	λ_{\max} (nm) (film)
1	1.16	755.0
2	6.10	782.8
10	2.58	624.2
11	18.00	653.8
16	5.20	642.4
18	1.44	630.2

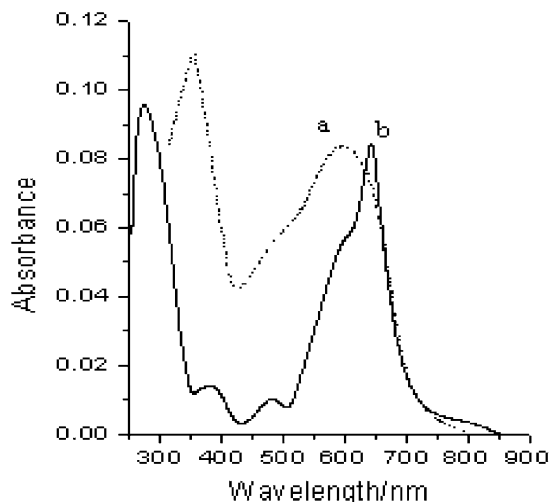


Fig. 5. Absorption of azo-metal chelates 11, 16 in film (a, for 16; b, for 11).

because of their excellent thermal and optical properties. The solubility of some azo-metal chelates in 4-hydroxy-4-methyl-2-pentanone and absorption maximum of their films were listed in Table 8. Some typical absorption spectra in the film were shown in Fig. 5. The results showed that the azo-metal chelates had good solubility in 4-hydroxy-4-methyl-2-pentanone, and they had a steep absorption at about 630–650 nm or about 780 nm. These properties made these azo-metal chelates had potential application for optical recording medium.

4. Conclusion

Some new azo dyes and azo-metal (Ni, Cr, Co) chelates were synthesized. The relationships between the difference of absorption maximum from azo-metal chelates to their ligands and the structures of the azo-metal chelates were studied. Some azo-metal chelates would be suitable for optical recording medium because of their good solubility and suitable absorption spectra in the thin film.

Acknowledgements

This work was supported by NSFC/China and Shanghai Scientific Technology Committee and Shanghai Education Committee.

References

- [1] Wang Sh-Sh, Tsaai H-P. US 2002091241, 2002.
- [2] Ueno Y, Sato T. JP 2002264519, 2002.
- [3] Tomura T, Noguchi T. JP 2002117589, 2002.
- [4] Azoma Y, Ueno Y. JP 2002144724, 2002.
- [5] Kurose H, Teruta T. JP 2002114922, 2002.
- [6] Sato T, Ueno Y. JP 2001180119, 2001.
- [7] Yamazaki K, Okubo N. JP 2002182419, 2002.
- [8] Watanabe K, Lwamoto Y. JP 200166543, 2001.
- [9] Chino T, Yamada M. JP 2001220519, 2001.
- [10] Tanaka M, Sakai T. JP 01104660, 1989.
- [11] Tanaka M. JP 02142855, 1990.
- [12] Yagi Y. Bull Chem Soc Japan 1963;36:487–92,500,506.
- [13] Yagi Y. Bull Chem Soc Japan 1964;37:1875–8.
- [14] Funatsukuri G. JP 41-20944, 1966.
- [15] Song J. US 27799683, 1957.
- [16] Choudaari SR, Goswami DD. J Indian Chem Soc 1978; LV:401–4.
- [17] Wang I, Hsu YH, Tian J. Dyes and Pigments 1991;16:83.
- [18] Yuki S, Michikazu H. US 6214519, 2001.